Contract No:

This document was prepared in conjunction with work accomplished under Contract No. DE-AC09-08SR22470 with the U.S. Department of Energy (DOE) Office of Environmental Management (EM).

Disclaimer:

SRNL-STI-2019-00022

Keywords: *Mechanical Properties, Type 304L Stainless Steel, Type 316L Stainless Steel, Type 21-6-9 Stainless Steel, Hydrogen Embrittlement, J-Integral, Helium Embrittlement*

Retention: Permanent

FRACTURE TOUGHNESS PROPERTIES OF TRITIUM-CHARGED-AND-AGED STAINLESS STEELS: SRNL AND SNL COLLABORATION TEST PLAN AND 2018 RESULTS

TIMOTHY M. KRENTZ[1], DALE A. HITCHCOCK[1], MICHAEL J. MORGAN[1], JOSEPH A. RONEVICH[2], RYAN SILLS[2], CHRIS SAN MARCHI[2], DORIAN K. BALCH[2]

[1]Savannah River National Laboratory, Energy Materials Group
[2]Sandia National Laboratories

Publication Date: February 2019

This document was prepared in conjunction with work accomplished under Contract No. DE-AC09-08SR22470 with the U. S. Department of Energy

Savannah River National Laboratory
Savannah River Nuclear Solutions, LLC
Aiken, SC 29808

Prepared for the U.S. Department of Energy under
contract number DE-AC09-08SR22470.

DISCLAIMER

This work was prepared under an agreement with and funded by the U.S. Government. Neither the U.S. Government or its employees, nor any of its contractors, subcontractors or their employees, makes any expressed or implied:

1. Warranty or assumes any legal liability for the accuracy, completeness, or for the use or results of such use of any information, product, or process disclosed; or
2. Representation that such use or results of such use would not infringe privately owned rights; or
3. Endorsement or recommendation of any specifically identified commercial product, process, or service.

Any views and opinions of authors expressed in this work do not necessarily state or reflect those of the United States Government, or its contractors, or subcontractors.

Printed in the United States of America

Prepared for
U.S. Department of Energy

Fracture Toughness Properties of Tritium-Charged-and-Aged Stainless Steels: SRNL and SNL Collaboration Test Plan and 2018 Results

Contents

TABLE OF FIGURES

TABLE OF TABLES

FRACTURE TOUGHNESS PROPERTIES OF TRITIUM-CHARGED-AND-AGED STAINLESS STEELS: SRNL AND SNL COLLABORATION TEST PLAN AND 2018 RESULTS

I. SUMMARY

Forged stainless steels are used as the materials of construction for tritium reservoirs. During service, tritium diffuses into the reservoir walls and radioactively decays to helium-3. Tritium and decay helium cause a higher propensity for cracking which could lead to a tritium leak or failure of a tritium reservoir. Fracture toughness properties are needed for designing tritium reservoirs and evaluating the long-term effects of tritium on their structural properties. A key result of prior studies is that the long-term cracking resistance of stainless steels in tritium service depends greatly on the interaction between decay helium and the steels' forged microstructure.

Designers and modelers at Sandia National Laboratories (SNL) have identified key gaps in the data available on material performance in tritium. Thus, a collaborative plan and schedule of tests have been developed with SRNL and SNL to fill these gaps using a range of tensile test and fracture mechanics test geometries, at stockpile relevant temperatures. These studies target the fundamental deformation mechanisms and the influence of tritium-decay-helium on their behavior. This report outlines the goals of each program and describes the sample test matrices and experimental conditions.

This report fulfills the requirements for a portion of the Enhanced Surveillance Campaign (ESC) FY19 Level 2 milestone 6725 to deliver an annual report on the aging studies of reservoir materials.

II. INTRODUCTION

Tritium reservoirs are constructed from forged stainless steels because of their acceptable tritium compatibility. These steels are resistant to, but not immune from, the embrittling effects of hydrogen isotopes and helium from tritium decay. Cracking in storage vessels has been observed after extended service times and material properties like ductility, elongation-to-failure, and fracture toughness are reduced with time as tritium and its radioactive decay product, He^3, accumulate within the vessel walls during service [1-8]. The factors that affect the tendency for crack formation and propagation include: (a) time of exposure; (b) steel type; (c) steel microstructure; (d) reservoir geometry and gas pressure; and, (e) reservoir residual stresses from welding and manufacturing.

Because of tritium aging effects, one of the primary interests of the Savannah River Site's Enhanced Surveillance program is to measure tritium effects on steel behavior and fracture toughness values for use by the Design Agencies (Sandia National Laboratories and Los Alamos National Laboratory) for fracture modeling, reservoir life prediction, and safety margin calculations [9-21]. This is especially critical as SRS is the only DOE facility capable of handling the necessary quantities of tritium to conduct these types of mechanical tests. Design Agencies, such as SNL, require fracture toughness properties for fracture mechanics analyses of pressure vessels and to provide designs that minimize the potential for tritium-induced crack growth. One of the key results of prior studies is that tritium compatibility, i.e., resistance to cracking and delayed failure, depends not only on the steel type, but on the steel microstructure.

Building on this history of testing, specific knowledge gaps have been identified in both engineering performance and mechanistic understanding of these material systems. Data are still missing on stockpile-relevant forgings, including the behavior of welds and heat affected zones, particularly for electron beam welds. Additionally, there is need for performance data on out of specification materials and materials at extremely advanced ages, with correspondingly high helium contents. For example, the SNL GTS design guide approves 304L stainless steel to helium contents of 1000 atomic parts per million, where limited data are available, and significant decreases in fracture toughness are seen in materials of this advanced age, as shown in Figure 1.

For future tritium reservoir design at SNL, computational modeling will play an increasingly important role. Models are only as good as the mechanistic understanding and material parameters on which they are founded, and data on these basic material properties is currently lacking. A systematic study on helium's effects on the deformation mechanisms in stainless steels is thus proposed by SRNL and SNL. It will address both room and low temperature behavior in model systems, including single- and oligo-crystals, to aid understanding of fundamental parameters. It will also investigate the emergent behavior of complex stress states that arise in constrained systems. These tests are selected to address gaps identified by designers and modelers at SNL.

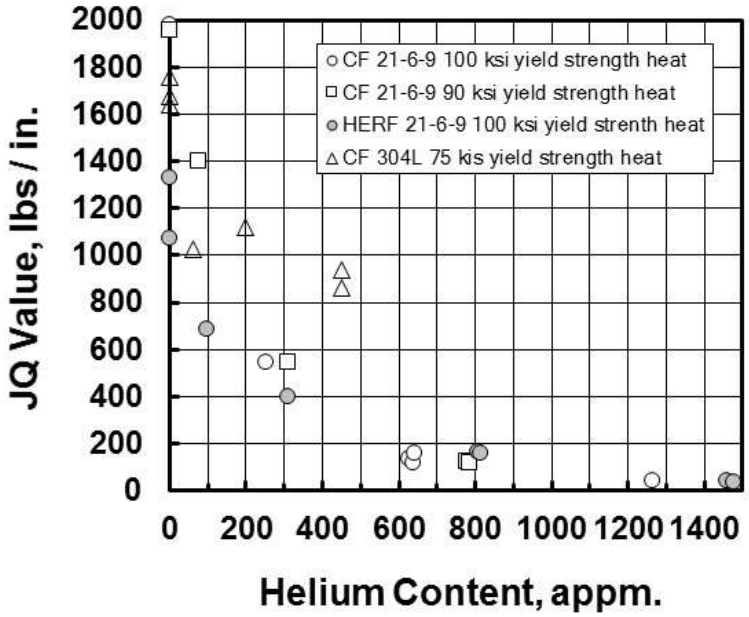

Figure 1 Fracture Toughness Reduction with Increasing Helium Content For Types 304L and 21-6-9 Stainless Steel Base Metals. Included are Data from Earlier Studies. Most Recent Data Shown are for Decay Helium Content Greater than 1000 appm [22].

Key gaps that have been identified include decay helium bubble size, spacing and distribution. These data are needed to develop fundamental deformation and cracking models for stainless steel. To that end, this report highlights initial results on the use of small angle neutron scattering (SANS) experiments on tritium-exposed-and-aged steels conducted at ORNL. Transmission electron microscopy (TEM) has been used to characterize helium bubble microstructures in tritium charged stainless steels [4, 11-13, 17] but the technique is unable to resolve bubbles that are smaller than 1 nm, nor can it easily resolve bubbles that are in heavily dislocated microstructures like the forged steels used in reservoirs. TEM will continue to be used where it is most effective - for characterizing small areas/volumes in welds, heat-affected zones and annealed steels. SANS should complement the TEM observations and provide data for more complex microstructures, as well as a broader statistical representation of the materials in question.

III. EXPERIMENTAL PROGRAMS

A series of new test programs, covering the next 5-10 years, are intended to address knowledge gaps in the effects of hydrogen, tritium, and decay helium on the mechanical performance of structural materials. In general, these programs are planned as multi-year efforts to build in relevant levels of helium, as calculated in Table 1.

Table 1 Calculated tritium decay helium levels assuming tritium charging at 350°C at 5ksi for 2 weeks with 304L

	0 yr	**0.48 yr**	**1.5 yr**	**3.1 yr**	**5.6 yr**
Tritium Conc (appm)	3724	3624	3424	3124	2724
Helium Conc (appm)	**0**	**100**	**300**	**600**	**1000**

Through collaborative discussions, SRNL and SNL have defined strategic test plans, outlined below, to address gaps in performance data and mechanistic understanding identified in tritium-material interactions and their impacts on mechanical behavior. These sets of experiments are designed to extract mechanical properties necessary to improve modeling and design of tritium containing components. Strategic experiments such as interrupted tests are designed to allow detailed microscopy to be performed at different stages of the deformation process. These represent the start of a coherent and comprehensive test plan assembled in collaboration between SRNL and SNL. It leverages SRNL's unique capabilities and expertise with tritium research and mechanical testing along with SNL's expertise in fracture mechanics and hydrogen effects on materials to support SNL's role to design reservoirs and to inform reservoir lifetime assessments. In these experiments, testing with hydrogen will be performed at SNL to establish a baseline understanding of mechanisms of hydrogen embrittlement, and testing with tritium will be performed at SRNL to understand the embrittlement mechanisms brought on by tritium and decay helium. Microscopy activities will be shared between both SRNL and SNL. These tests are listed in roughly priority order, with the first half also corresponding chronologically to yearly charging runs. Studies further down the list are still in development but carry significant impact for future reservoir design.

The programs are:

1. 304L Tube tensile tests
2. 304L Notched tensile tests
3. 304L and 21-6-9 Smooth tensile tests at room and low temperature
4. 304L E-beam weld fracture mechanics and tensile tests at room and low temperature
5. Stainless Steel single crystal tensile tests
6. Stainless steel oligocrystal tensile tests
7. 304L forge/weld/HAZ low temperature fracture tests
8. Aluminum tensile and fracture tests
9. Static load stainless steel and aluminum tests

The next section of the report outlines the goals of each program and describes the sample test matrices, experimental conditions, and testing schedules specifically for tests performed at SRNL with tritium. These test plans are meant to serve as a roadmap which may evolve over time but provide a foundation for planning. The experimental procedures that will be used are described in subsequent sections.

1. 304L Tube Tensile Testing

Several years ago, SNL performed a series of heat treatments on 304L stainless steel tubes to examine the role that strength/microstructure has in hydrogen-sensitivity. The purpose behind this work is to address effects of non-conformance components. The tensile curves from this work are shown in Figure 2 [23-25]. The purpose of this program is to measure the interactions of hydrogen, tritium, and decay helium with varying strengths as well as differing dislocation and grain structures but with the same nominal composition. Differing annealing temperatures and welds allow for a variety of microstructures to be generated from the same 304L stainless steel tube, which have been shown at SNL to have significant impact on the stress strain behavior with hydrogen charging. The proposed test matrix is shown in full in Table 2.

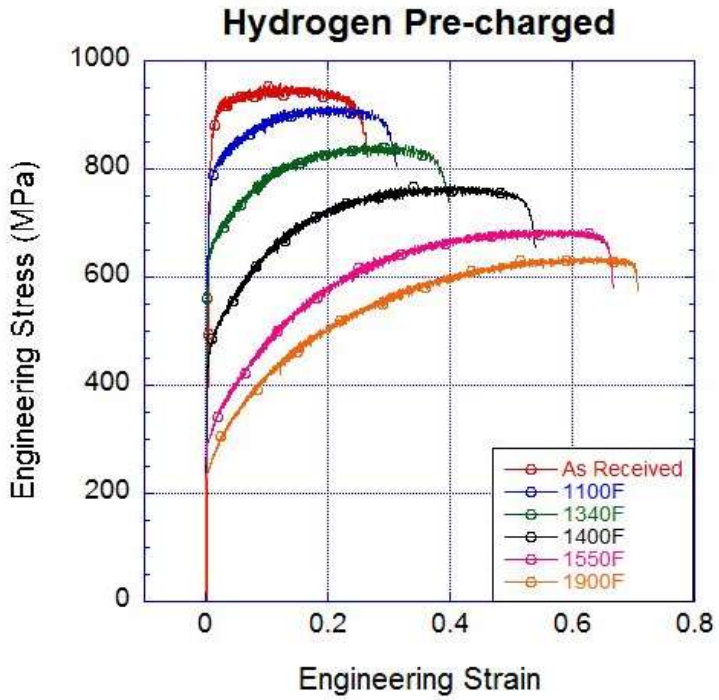

Figure 2 Stress/Strain curves from hydrogen charged 304L tubes annealed at various temperatures (curves are unpublished but represent data reported in [23-25])

Table 2 Tube Tensile test matrix

Microstructure	**Numbers of specimens**		
	100 ppm He (~6mo)	**300 ppm He (1.5 yr)**	**600 ppm He (3 yr)**
As received	2	2	2
As-received welds	2	2	2
1100F	2	2	2
1340F	2	2	2

1340F welds	2	2	2
1400F	2	2	2
1550F	2	2	2
1900F	2	2	2
1900F welds	1	2	2

2. 304L Notched Tensile Testing

The purpose of this program is to measure the effect of tritium and decay helium on notch strength in complex stress states. The notched geometry creates a central region of increased stress intensity whose volume is significantly larger than the stress concentrator around the crack tip in fracture mechanics specimens. Thus, interrupted tensile tests with these types of specimens can be used to examine void nucleation and growth via metallographic inspection post-test. The stress riser of the notch is approximately a K_t of 2, and the full geometry of the samples is shown in Figure 3. The proposed test matrix is shown in full in Table 3. Note, the interrupted strains will be determined by the flow curves following test to failure.

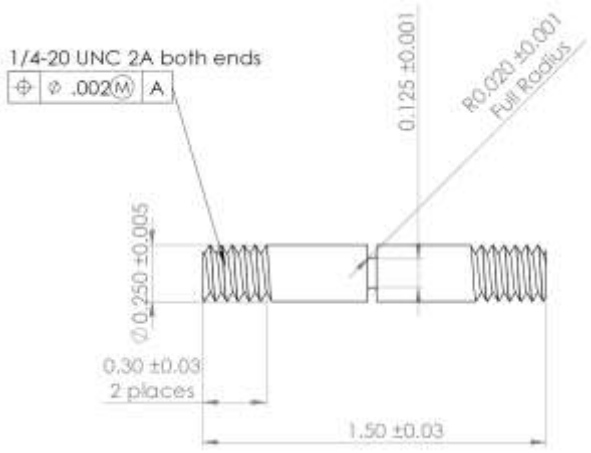

Figure 3 Schematic of notched tensile specimen

Table 3 Notched tensile test matrix

	Number of specimens		
	100 appm He (6 mo)	300 appm He (1.5 yr)	600 appm He (3 yr)
Failure	2	2	2
Interrupted strain 1	2	2	2
Interrupted strain 2	2	2	2

3. 304L & 21-6-9 Smooth tensile testing

The purpose of this program is to create flow curves to inform computational models being developed for future reservoir design. This test comprises several strain levels of interrupted tests; a low strain (5%), moderate strain (20%), a strain just below failure (failure -5%), and to failure. These are shown in Table 4. Each test will be conducted at both ambient (23°C) temperature and reduced (-50°C) temperature for each alloy. These interrupted tests can be interrogated to provide information on tritium and helium's effects on deformation processes in stainless steel alloys, as well as the effects of temperature on these mechanisms. Baseline tests in the H-precharged condition will be reported in [25]. Low temperature tests may reveal changes in dislocation slip due to reduced hydrogen diffusivity and increasing quantities of helium bubbles. Finally, as above, tests run just shy of failure will hopefully provide metallographic information on void nucleation and growth behaviors in tritium/helium embrittled steels.

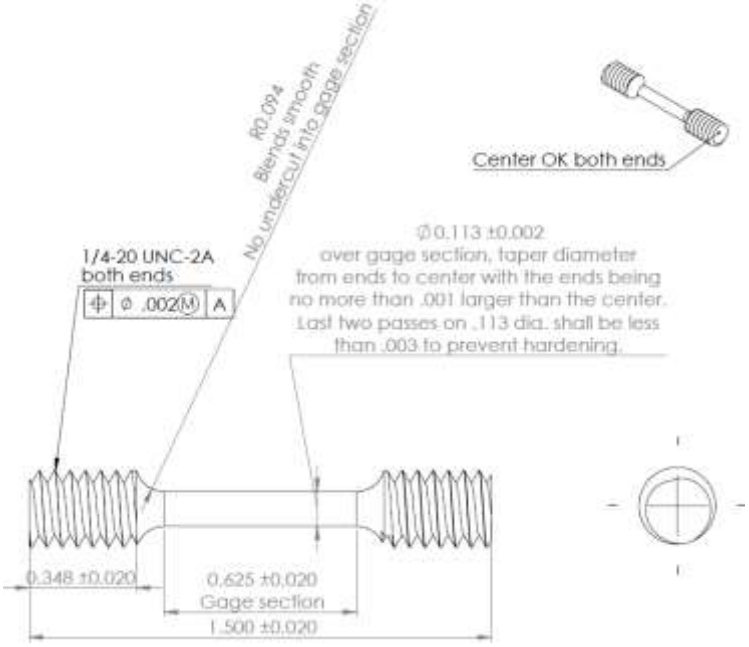

Figure 4 Schematic of smooth tensile specimen

Table 4 Smooth tensile test matrix

		Number of specimens			
		100 appm He (6 mo)*	300 appm He (1.5 yr)*	600 appm He (3 yr)*	1000 appm He (5.6 yr)*
Aged then tested	Failure	3	3	3	3
	5% (true strain)	2	2	2	2
	20% (true strain)	2	2	2	2
	Failure -5% (true strain)	2	2	2	2

4. 304L forgings with E-beam welds

The purpose of this program is to create flow curves to inform computational models being developed for future reservoir design, specifically on the increasingly prevalent electron beam welds being used on future reservoirs. There exists relatively little data on the behavior of these materials in tritium conditions, and thus two basic series of tests would be performed: tensile and fracture mechanics. Tensile specimens would be the same as shown in Figure 4, except containing E-beam welds. For fracture testing, the sample of choice at SRNL has been the Arc specimen shown in Figure 5, which will also be used in these studies. Previous work at SRNL and SNL has demonstrated the ability to deliberately localize fracture in the weld and in the heat affected zone, both of which will be investigated in this study. Both tensile and fracture tests are important to characterize the poorly understood structural and property ramifications of this weld process. The full test matrices for tensile and fracture testing of E-beam welds are detailed in Table 5 and Table 6, respectively.

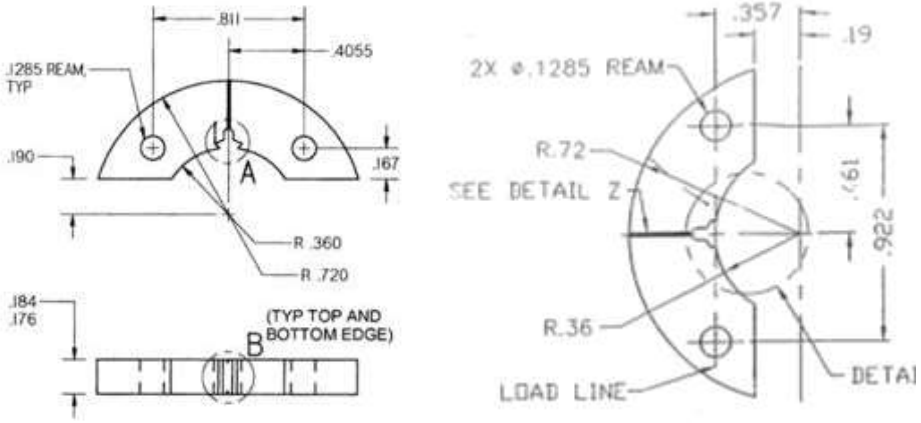

Figure 5 Schematic of fracture mechanics Arc specimen, units in inches

Table 5 304L E-beam weld tensile test matrix

	Number of specimens			
	100 appm He (6 mo)	300 appm He (1.5 yr)	600 appm He (3 yr)	1000 appm He (5.6 yr)
Failure (23°C)	2	2	2	2
Failure (-50°C)	2	2	2	2

Table 6 304L E-beam weld fracture test matrix

	Number of specimens			
	100 appm He (6 mo)	300 appm He (1.5 yr)	600 appm He (3 yr)	1000 appm He (5.6 yr)

Failure (23°C)	2	2	2	2
Failure (-50°C)	2	2	2	2

5. Single Crystal tensile tests

SNL has been pursuing work on single and oligo ("having a few") crystals precharged with hydrogen to try and pursue a fundamental understanding of how the presence of hydrogen changes deformation mechanisms. Preliminary tests with single crystal nickel were conducted at SNL, with samples as shown in Figure 6 and the resulting data in Figure 7. Further tests are under way at SNL with several orientations of 316L single crystal samples, with and without hydrogen charging. This program will extend this work to tritium and decay helium on austenitic stainless steel single and oligo crystals. A full test matrix for this study is pending SNL's results in hydrogen but will likely involve several of the typical ages listed in the studies above, with ambient and sub-ambient temperatures, for each of a few crystallographic orientations. These types of tests will aid in informing mechanistic models of deformation, improving capabilities and confidence in their use for reservoir design.

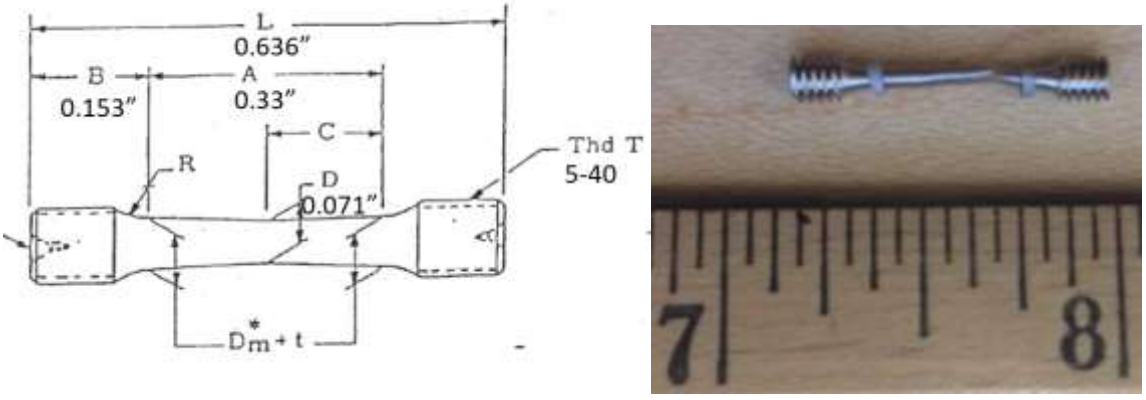

Figure 6 Schematic and image post-test of samples being used for preliminary testing at SNL in hydrogen pre-charged condition

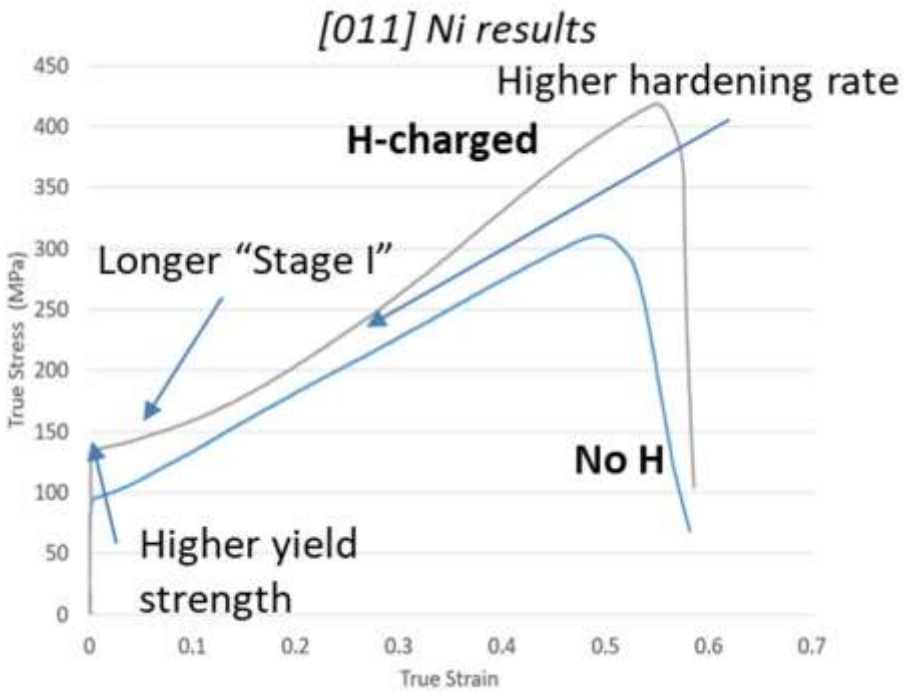

Figure 7 Preliminary single crystal [011] tensile test results in nickel with and without hydrogen charging performed at SNL.

6. Oligocrystals

SNL has developed an annealing process to produce controlled oligocrystal tensile specimens (see micrograph in Figure 8). These large grains provide a means of extracting small tensile specimens with just a few grains in the gage section. A test matrix like that described above for single crystals will be performed on these oligocrystal specimens. Digital image correlation (DIC) techniques may also be used to create high resolution strain maps, allowing for the empirical validation of Crystal Plasticity models being developed by the computational mechanics group at SNL. The SRNL team is exploring options for developing DIC techniques that can be implemented during testing for tritium-precharged specimens, more development will be needed to perform DIC in tritium precharged materials.

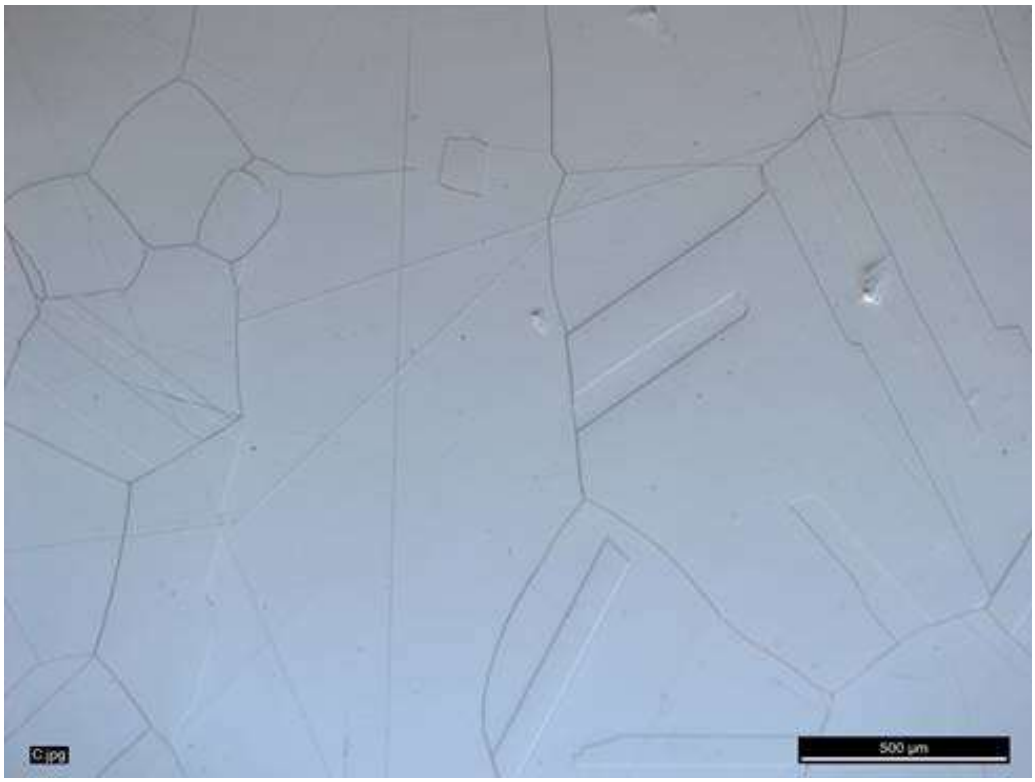

Figure 8 304L oligocrystal sample after annealing at 1150°C for 24 hours, developed by SNL.

7. Low Temperature Fracture toughness

Previous work performed at SNL [26] on hydrogen precharged stainless steel welds, showed unique response at low temperature depending on the weld. Three different welds were fabricated at SNL using 308L filler from three different forgings: 304L, 21-6-9, and 316L. Following hydrogen precharging, the 304L and 21-6-9 welds showed negligible effects of low temperature, whereas the 316L welds exhibited a 50% reduction in fracture toughness, as shown in Figure 9. In order to evaluate the entire STS range, fracture toughness experiments should be performed at both temperatures and further research is needed in both hydrogen and tritium precharged conditions. Test plans are still under development to determine what specific welds we would like to examine at -50°C.

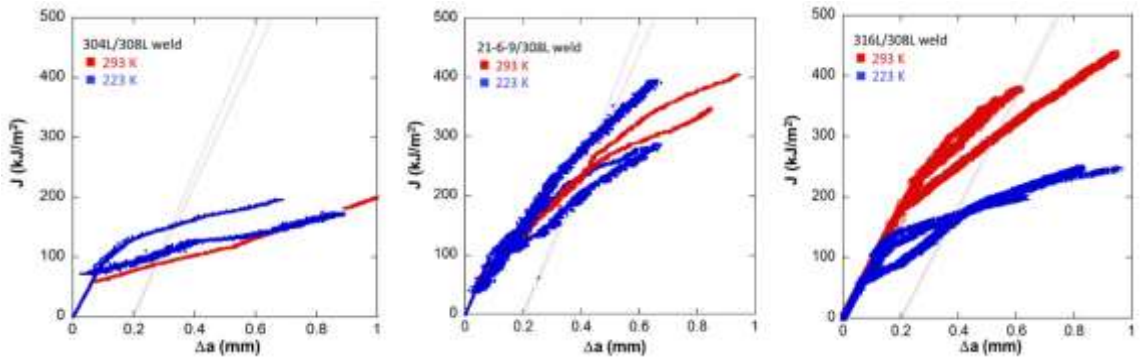

Figure 9 Hydrogen charged 304L, 21-6-9, and 316L welds fabricated with 308L filler metal tested for fracture toughness at ambient and low temperature [26]

8. Aluminum testing

2219 Aluminum alloy (an aluminum/copper precipitation hardening alloy, nominal composition shown in Table 7) has been selected as a structural material for future reservoirs, however, no data are available on the long term mechanical performance of aluminum exposed to tritium conditions. Aluminum is not expected to display the same levels of embrittlement as ferrous alloys due to a lower solubility for hydrogen, however, detailed studies are needed to fully understand the behavior of tritium in 2219 aluminum alloys.

Low temperature charging conditions will be necessary to prevent unwanted aging of the alloy's precipitate microstructure. Because of the aluminum oxide surface layer's propensity to adsorb hydrogen and hydrogen isotopes, there will be additional challenges associated with a relatively high activity of the samples compared to all prior testing in ferrous alloys. A full test plan pends initial successful trials to prove out effective charging conditions and the evaluation of test procedures that are both relevant, and radiologically practical. Tensile and fracture behavior are of interest for this study.

Table 7 Nominal Composition of 2219 aluminum alloy

Al	Cu	Fe	Mg	Mn	Si	Ti	V	Zi	Zr	Residuals
Balance	5.8-6.8	<0.3	<0.02	0.2-0.4	<0.2	0.02-0.1	0.05-0.15	<0.1	0.1-0.25	<0.15

9. Static Loading testing

The final test program described in this report is focused on simulating what a pressurized reservoir experiences in terms of the loading environment. To do this, it will make use of a wedge-open loaded (WOL) static load crack growth test. A sample is shown in Figure 10. Samples would be precharged with tritium and a fixed displacement would be applied. They would be allowed to age under stress and in a tritium atmosphere, building in decay helium with a sustained strain field in the sample. This will provide

information on how tritium and helium bubbles distribute under a load, providing data relevant to reservoirs which sustain a static load throughout service.

Figure 10 Wedge Open Loaded (WOL) static load crack growth test sample with strain gauge attached

IV. EXPERIMENTAL PROCEDURE

For each of the programs, samples will be pre-charged with either hydrogen or tritium gas at 623 K and an over-pressure of 34.5 MPa and then stored in air at 193K. The storage temperature is chosen to minimize tritium off-gassing losses and allow for the build-in of helium from tritium decay until testing is performed. The amount of helium in each sample on the date of each test will be back calculated from initial tritium contents. Selected samples may have tritium and helium contents measured via thermal desorption spectroscopy. The hydrogen isotope content of the pre-charged samples will be approximately 3700 atomic parts per million (appm) for Types 304L and 316L stainless steels and 6300 appm for Type 21-6-9 stainless steel by using established hydrogen solubility values [27]. Helium contents will depend on the steel type and aging conditions and will range between 0 appm and 1000 appm.

Most of the fracture mechanics testing will be J-integral tests conducted at room temperature in air using a screw-driven testing machine and a constant crosshead speed while recording load, load-line displacement with a gage clipped to the crack mouth, and crack length (see Figure 11). Crack length will be monitored using a DC potential drop system and guidelines described in ASTM E647-95 [28]. The J-Integral versus crack length increase (J-R) curves will be constructed from the data using ASTM E1820-99 [29]. Tensile tests will be conducted on the same load frame, with grips appropriate to the samples shown in schematic in earlier sections. Load and extension data will be gathered. Crosshead speed may be varied test-to-test to investigate effects of strain rate on fracture toughness and tensile response. Some of the tests will be conducted at sub-ambient temperatures (-50°C). SRNL is exploring options to develop low temperature testing capability for tritium-charged specimens.

Figure 11 shows the typical sample configuration for fracture toughness measurements that will be used. Figure 12 shows a typical result from earlier work at SRNL on the effect of hydrogen and tritium on fracture toughness properties of Type 21-6-9 stainless steel [18]. Two rising-load fracture toughness parameters will be determined from the tests. First, the fracture toughness value, J_Q, as specified by ASTM 1820 will determined from the intercept of the J-R curve with the 0.2 mm offset line [29]. A rising-load, cracking-threshold value, J_{TH}, will be determined also using a 0.05 mm offset, which is apparently closer to the actual point of crack extension in these steels as indicated by tritium release and the DC potential drop measurements [21].

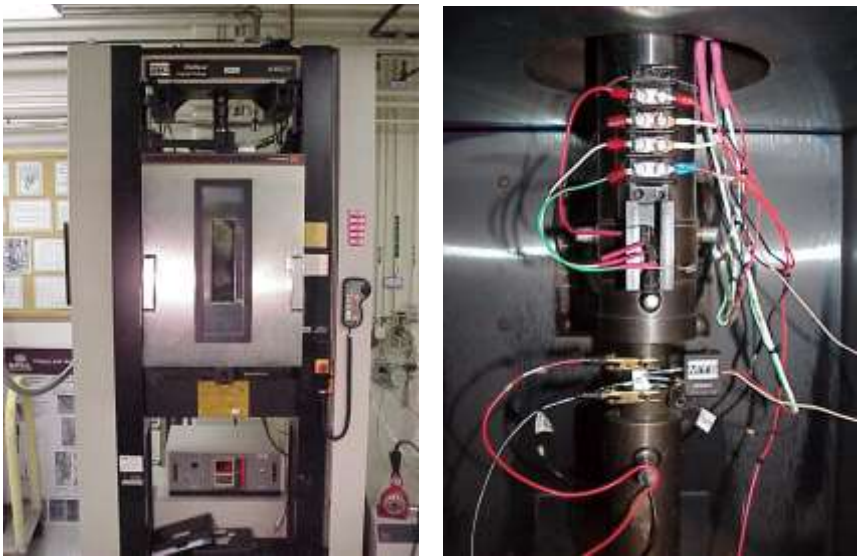

Figure 11 (a) Mechanical testing machine with environmental chamber for non-charged and hydrogen-charged samples. **(b)** Fracture-toughness sample with crack length DC potential drop leads and thermocouple. A similar chamber and sample configuration will be used for tritium tests.

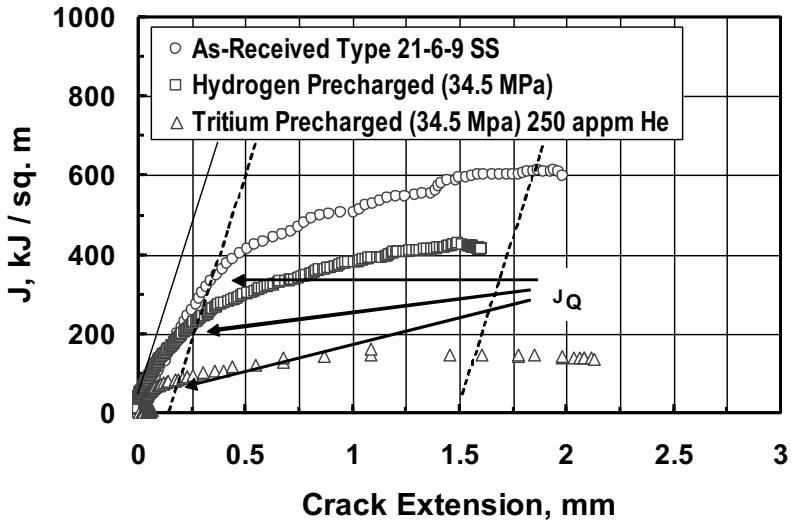

Figure 12 Typical J-R curves for as-received (Not Charged), Hydrogen pre-charged, and Tritium pre-charged Type 21-6-9 stainless steels. J_Q values shown were determined from the intercept of the J-R curve with the 0.2 mm offset line. J_{TH} values (Not Shown) were determined using a 0.05 mm offset line.

V. SMALL ANGLE NEUTRON SCATTERING RESULTS

At the end of 2017, SRNL prepared samples for study via small angle neutron scattering (SANS) at ORNL. The purpose is to learn as much as possible about decay helium bubble size, spacing and distribution to support deformation and cracking models for stainless steel. Transmission electron microscopy has been used to characterize helium bubble microstructures in tritium charged stainless steels [8, 15], but the technique is unable to resolve bubbles that are smaller than 1 nm, nor can it easily resolve bubbles that are in heavily dislocated microstructures like the forged steels used in reservoirs. TEM will continue to be used where it is most effective - for characterizing small areas/volumes in welds, heat-affected zones and annealed steels. SANS should complement the TEM observations and provide data for more complex microstructures, as well as a broader statistical representation of the materials in question.

Neutron scattering measurements were performed on tritium exposed stainless steel samples on beamline CG-2 at the High Flux Isotope Reactor (HFIR) at Oak Ridge National Lab (ORNL), shown in Figure 13. The measurements were performed during one day of beamtime (12/2/17) granted through the general user proposal process. Two types of measurements were performed. Small angle neutron scattering (SANS) measurements were performed to elucidate the nature of Helium bubble formation in the matrix, and small angle incoherent neutron scattering (SAINS) measurements were performed to measure the hydrogen content in the samples.

Figure 13 the General-Purpose SANS instrument, detector in the left of the two vacuum chambers, at HFIR at ORNL

The samples chosen for the study are detailed in Table 8 below. The samples were chosen to study similar tritium exposed stainless steels aged for different times, as well as the effect of weldments on the formation of helium bubbles and hydrogen retention.

Table 8 Samples prepared for SANS measurement

Sample	Charging	Age
304/308 filled steel weldments	T2	17-year
high energy rate forged 304	T2	3-year
304/308 filled steel weldments	H2 (5000psi)	N/A
304/308 filled steel weldments	H2 (10000psi)	N/A
304L/308 filled steel weldment	uncharged	N/A
High energy rate forged 304 steel	uncharged	N/A

Prior to performing the measurements, the samples were machined from previously studied fracture toughness specimens at SRNL using both hot (tritium-exposed) and clean EDM facilities. Shown in Figure 14 a) the geometry of the neutron scattering samples was chosen to maximize the cross section from the available fracture toughness specimens. The SANS samples Figure 14 b) were also cut to 0.5mm thick to minimize multiple scattering during the neutron measurements. Additionally, a sample cell was developed for the tritiated samples to allow them to be handled openly in the low rad areas of the neutron facility. The cell consisted of two zero length ConFlat viewports (1.33” dia.) for confinement and an Aluminum washer to hold the samples in place (Figure 14 c/d). The viewport is made of high purity quartz to minimize scattering of the

incident neutrons. The tabs on either side of the sample are designed to fit in a trough machined into the aluminum washer to ensure the sample position does not vary during the measurements. Figure 14 c) shows the cell loaded with the Aluminum washer but no sample.

The tritium-precharged samples inside their cells were shipped in a DOT approved container. Prior to shipment calculations were performed to show that the activity was below the DOT limits, and all surfaces of every layer of the packaging were monitored for contamination prior to shipment. Importantly the sample cells ensured that no contamination could be transferred to the packaging. Finally, after arrival at Oak Ridge additional rad con surveys confirmed that no contamination was present anywhere on the package or on the outside of the sample cells.

Measurements were performed using a 2.5mm beam spot to allow for measurements in the HAZ and as-forged regions of welded samples. SANS and basic static SAINS measurements were performed on all the samples, and on both sides of the weld containing samples. On the protium containing welded samples, additional scanning SAINS measurements were performed scanning across the weldment in 0.1mm steps.

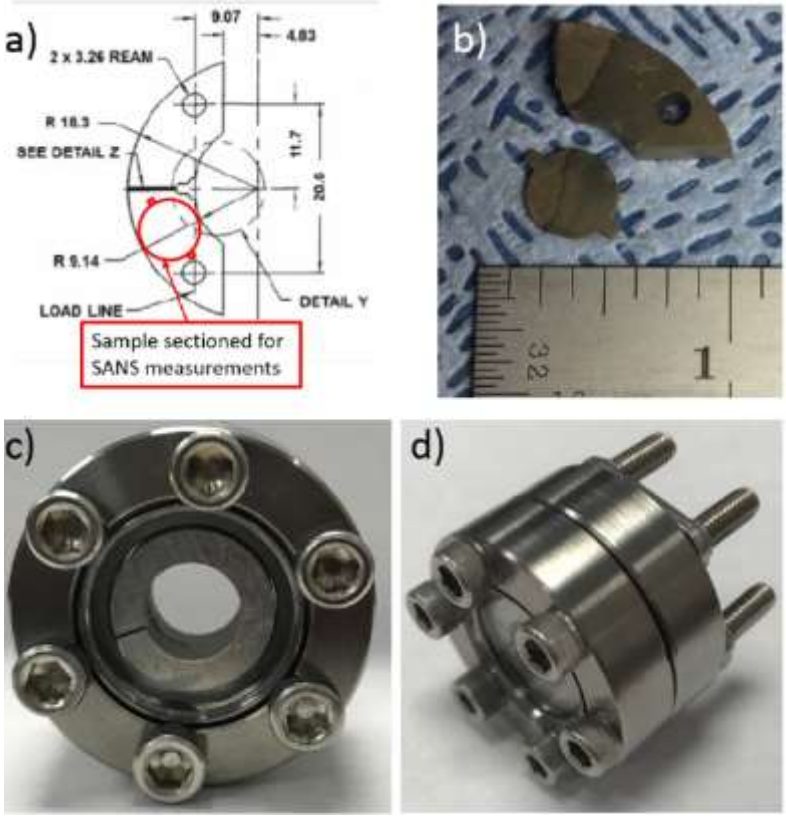

Figure 14 a) diagram of the geometry of the SANS samples machined from previously studied fracture toughness specimens at SRNL, b) picture of a SANS sample (note: the variation in color across the sample corresponds to regions of weld and base metal) c/d) samples cells designed for use in the neutron facility

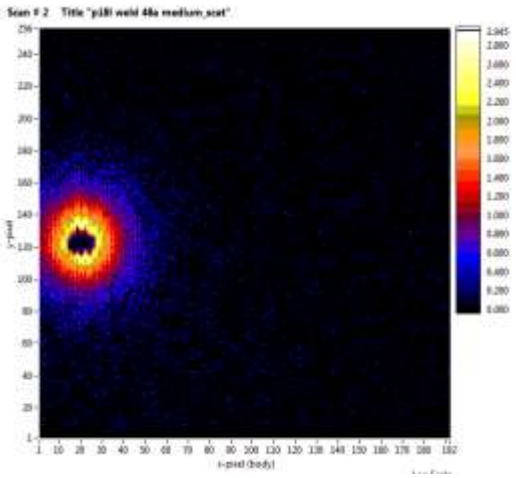

Figure 15 Prototypical raw 2D map of scattering data

Figure 15 is a 2D map showing the raw data from one measurement. Data analysis has revealed that sample thicknesses were overly conservative, and slightly thicker samples can be employed in future SANS measurements to maximize the scattering signal while still avoiding multiple scattering events. This two-dimensional dataset is reduced via azimuthal summation, giving data of intensity versus Q (related to angle by the energy of the incident neutrons). An example is shown in Figure 16.

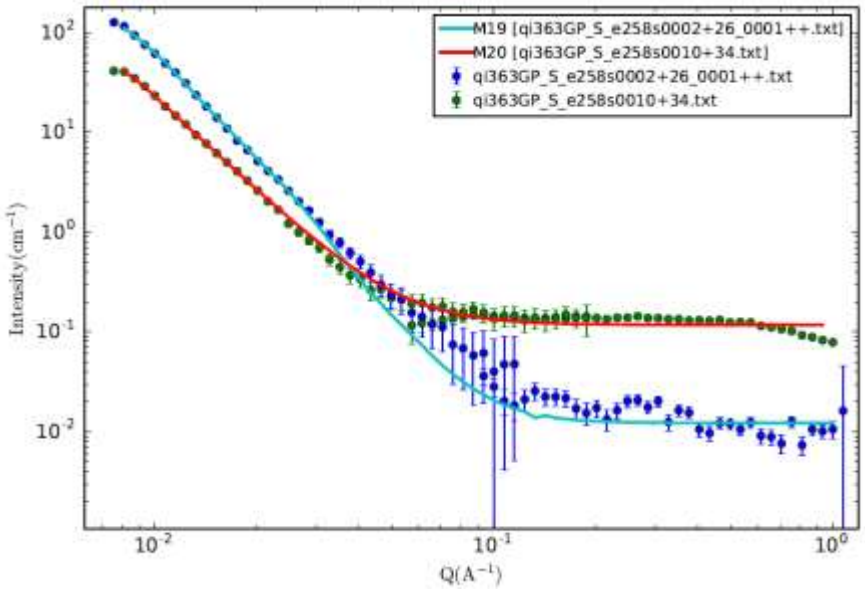

Figure 16 Reduced and fitted data from a hydrogen charged weld (green with red fit) and tritium charged weld aged 3 years (blue with light blue fit).

From the reduced and fitted data, several observations can be made. In Figure 16, two separate fitting functions are used. For the hydrogen charged weld, it is well fit by a Gunier-Porod model, with the bulk of the scattering due to the complex microstructure of the weld sample. However, in the tritium charged and aged sample, significant additional

scattering can be seen which is well fit by a hard sphere model. In fitting this sample, the two most interesting parameters are the radius of gyration, corresponding to the average bubble size, and the scattering length density, which directly relates to the helium pressure inside the bubbles. In this fit, a radius of gyration of 2.3 nanometers and a pressure of ~3 GPa were used, which confirm other measurements in the literature, and match closely to observations from TEM micrographs.

One more observation to be made from these data is in the background at high Q. The hydrogen charged sample exhibits 10-20 times as much incoherent scattering background as the tritium charged sample, despite nominally identical hydrogen isotope concentrations. This might be attributed to two combined effects: the decay of tritium in 17 years will have reduced concentrations by more than a factor of 2 (tritium half-life = 12.3 years) and additionally, protium has an incoherent scattering cross section substantially higher than tritium. Because this background represents an additional source of information, an additional series of measurements were conducted in the form of SAINS scans across these welds. A short measurement was taken at a series of locations linearly across each weld, and the background can be summed into a measure of total counts at each location. This technique follows work from ORNL [30]. The scans for clean, protium charged, and tritium charged weld samples are shown in Figure 17.

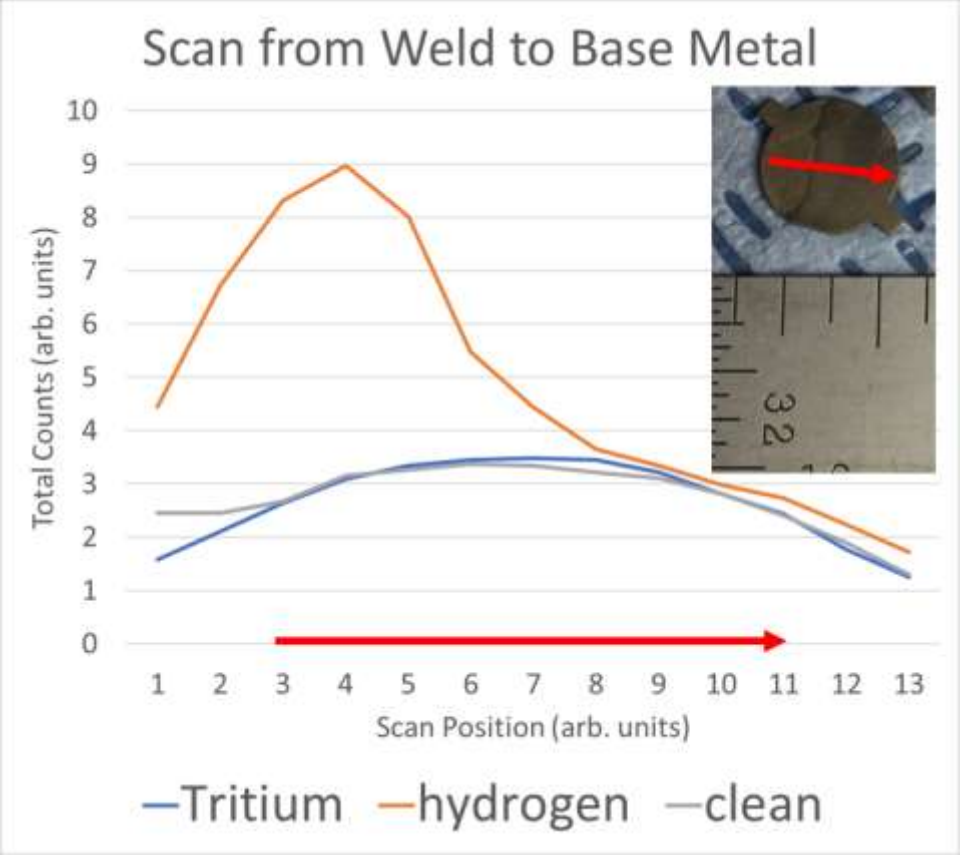

Figure 17 Summed SAINS measurements conducted in a scan across weld (direction shown in insert)

VI. CONCLUSIONS

An experimental test plan has been developed between SRNL and SNL to provide data that fills important gaps in knowledge on the effects of tritium on stainless steels. The test plan will employ a range of tensile test and fracture mechanics test geometries, at stockpile relevant temperatures. The plan will provide data that elucidates the fundamental deformation mechanisms and the influence of tritium-decay-helium on their behavior. To do that tensile tests on smooth and notched geometries will be conducted along with comprehensive microstructural examinations of interrupted tests. These examinations will include transmission electron microscopy at SNL and SRNL to characterize helium bubble microstructures as a function of stress and strain states and age. Neutron scattering will also be conducted to provide better statistical characterization of bubble size, spacing, and possibly pressures. This report outlines the goals of each program and describes the sample test matrices and experimental conditions. Preliminary results from SANS measurements were also described, which agree with historical TEM examinations on helium bubble size, as well as indicating that further spatially resolved measurements of hydrogen isotope content and bubble microstructure may be possible with further technique development, planned for upcoming fiscal years.

REFERENCES

1. Caskey, G.R., *Hydrogen Effects in Stainless Steel*, in *Hydrogen Degradation of Ferrous Alloys*, R.A. Oriani, J.P. Hirth, and M.A. Smialowski, Editors. 1985, Noyes Publishing: Park Ridge, NJ. p. 822-862.
2. Robinson, S.L., *The Effects of Tritium on the Flow and Fracture Stress of Austenitic Stainless Steels*, in *Hydrogen Effects on Material Behavior*, N.R. Moody and A.W. Thompson, Editors. 1990, TMS: Warrendale PA. p. 433-445.
3. Robinson, S.L. and G.J. Thomas, *Accelerated Fracture due to Tritium and Helium in 21-6-9 Stainless Steel.* Metallurgical Transactions A, 1991. **22A**: p. 879-885.
4. Morgan, M.J. and M.H. Tosten, *Tritium and decay helium effects on the fracture toughness properties of types 316L, 304L and 21Cr-6Ni-9Mn stainless steels*, in *Hydrogen Effects in Materials*. 1996, TMS: Warrendale, PA. p. 873-882.
5. Morgan, M.J. *Tritium Aging Effects on the Fracture Toughness Properties of Forged Stainless Steels*. in *Proceedings of the Conf. on Materials Innovations in an Emerging Hydrogen Economy*. 2008. Cocoa Beach, Florida, USA.
6. Morgan, M.J. *Hydrogen Effects on the Fracture Toughness Properties of Forged Stainless Steels*. in *Proceedings of PVP2008 ASME Pressure Vessels and Piping Division Conference*. 2008. Chicago Illinois, USA.
7. Morgan, M.J., S.L. West, and M.H. Tosten. *Effect of Tritium and Decay Helium on the Fracture Toughness Properties of Stainless Steel Weldments*. in *Proceedings of the 8th Int. Conf. on Tritium Science and Technology,*. 2008. Rochester, NY, USA: Fusion Science and Technology.
8. Tosten, M.H. and M.J. Morgan. *Transmission Electron Microscopy Study of Helium Bearing Fusion Welds*. in *2008 Int. Hydrogen Conf. - Effect of Hydrogen on Materials*. 2009. Materials Park, OH: ASM International.
9. Morgan, M.J. *THe Effects of Hydrogen Isotopes and Helium on the Flow and Fracture Properties of 21-6-9 Stainless Steel*. in *Proc. Fine Symposium*. 1990. Warrendale, PA: TMS.
10. Morgan, M.J. and D. Lohmeier, *Threshold Stress Intensities and Crack Growth Rates in Tritium-Exposed HERF Stainless Steels*, in *Hydrogen Effects on Material Behavior*, N.R. Moody and A.W. Thompson, Editors. 1990, TMS: Warrendale PA. p. 459-468.
11. Morgan, M.J. and M.H. Tosten. *Microstructure and Yield Strength Effects on Hydrogen and Tritium Induced Cracking in HERF Stainless Steel*. in *Hydrogen Effects on Material Behavior*. 1990. Warrendale PA, USA: TMS.
12. Morgan, M.J. and M.H. Tosten, *Tritium and decay helium effects on the fracture toughness properties of types 316L, 304L and 21Cr-6Ni-9Mn stainless steels*. 1994, Westinghouse Savannah River Co.: Aiken.
13. Morgan, M.J. and M.H. Tosten, *Tritium and decay helium effects on cracking thresholds and velocities in stainless steel.* Fusion Technology, 2001. **39**: p. 590-595.
14. Kim, Y., et al., *C-Specimen Fracture Toughness Testing: Effect of Side Grooves and eta Factor.* Journal Of Pressure Vessel Techology, 2004. **160**: p. 293.
15. Tosten, M. and M. Morgan, *Transmission Electron Microscopy Study of Helium Bearing Fusion Welds WSRC-TR-2005-00477*. 2005, Savannah River National

Laboratory, Washington Savannah River Company, Savannah River Site: Aiken, SC.
16. Tosten, M.H. and M. M.J., *Microstructural Study of Fusion Welds in 304L and 21Cr-6Ni-9Mn Stainless Steels WSRC-TR-2004-00456*. 2005, Savannah River National Laboratory, Washinton Savannah River Company: Savannah River Site, Aiken, SC, USA.
17. Morgan, M.J. and M.H. Tosten, *Tritium Effects on Weldment Fracture Toughness*. 2006, Savannah River National Laboratory, Washington Savannah River Company: Savannah River Site, Aiken, SC, USA.
18. Morgan, M.J. and G.K. Chapman, *Hydrogen Effects on the Fracture Toughness Properties of Type 316L Stainless Steel WSRC-TR-2007-00479*. 2007, Savannah River National Laboratory, Washington Savannah River Company: Savannah River Site, Aiken SC, USA.
19. Morgan, M.J. and G.K. Chapman, *Hydrogen Effects on the Fracture Toughness properties of Type 316L Stainless Steel from -100C to +150C SRNL-TR-2008-00317*. 2008, Savannah River National Laboratory: Aiken, SC, USA.
20. Morgan, M.J. and G.K. Chapman, *Hydrogen Effects on the Fracture Toughness Properties of Types 304L and 21-6-9 Stainless Steels from 173K to 423K*. 2009, Savannah River National Laboratory, Washington Savannah River Company: Aiken, SC, USA.
21. Morgan, M.J. and G.K. Chapman, *Cracking Thresholds and Fracture Toughness Properties of Tritium Charged and Aged Stainless Steels WSRC-TR-2010-00393*. 2010, Savannah River National Laboratory, Washington Savannah River Company: Aiken, SC, USA.
22. Morgan, M.J., et al., *2017 Accomplishments–Tritium Aging Studies on Stainless Steel Weldments and Heat-Affected Zones*. 2018, Savannah River Site (SRS), Aiken, SC (United States).
23. Hughes, L.A., et al., *Hydrogen compatibility of austenitic stainless steel tubing and orbital tube welds.* International Journal of Hydrogen Energy, 2014. **39**(35): p. 20585-20590.
24. Hughes, L.A., et al. *Hydrogen Compatibility of Austenitic Stainless Steel Tubing and Orbital Tube Welds*. in *International Conference on Hydrogen Safety (ICHS)*. 2013. Brussels, Belgium.
25. San Marchi, C., et al. *Effect of Microstructural and Environmental Variables on Ductility of Austenitic Stainless Steels*. in *International Conference on Hydrogen Safety*. 2019. Adelaide, Australia.
26. Ronevich, J.A., C. San Marchi, and D.K. Balch. *Temperature Effects on Fracture Thresholds of Hydrogen Precharged Stainless Steel Welds*. in *ASME 2017 Pressure Vessels and Piping Conference*. 2017. American Society of Mechanical Engineers.
27. San Marchi, C.S., B.P. and S.L. Robinson, *Permeability, Solubility, and Diffusivity of Hydrogen Isotopes in Stainless Steels at High Gas Pressures.* International Journal of Hydrogen Energy, 2007. **32**: p. 100-116.
28. *ASTM E647-95a Standard Test Method for MEasurement of Fatigue Crack Growth Rates*, in *1999 Annual Book of ASTM Standard Volume 3.01 Metals-Mechanical Testing; Elevated and Low-Temperature Tests; Metallography*. 1999.

29. *ASTM E1820-99 "Standard Test Method for Measurement of Fracture Toughness"*, in *1999 Annual Book of ASTM Standards Volume 3.01: Metals-Mechanical Testing; Elevated and Low-Temperature Tests; Metallography;*. 1999, American Society for Testing and Materials.
30. Yan, Y.Q., S; Littrell, K; Parish, C M; Plummer, L K, *Fast, quantitative, and nondestructive evaluation of hydrided LWR fuel cladding by small angle incoherent neutron scattering of hydrogen.* Journal of Nuclear Materials, 2015. **460**: p. 114-121.